Epoxidized Styrene–Butadiene–Styrene Block Copolymer Membrane Complexes with Cobalt Schiff Bases for Oxygen Permeation

Jen-Ming Yang and Ging-Ho Hsiue*

Department of Chemical Engineering, National Tsing Hua University, Hsinchu, Taiwan 30043, R.O.C.

Received August 24, 1990; Revised Manuscript Received November 12, 1990

ABSTRACT: The complex formation of epoxidized styrene–butadiene–styrene triblock copolymer (ESBS) with cobalt Schiff base (CoS) in chloroform solution is studied. Facilitated transport of molecular oxygen in ESBS membranes containing various cobalt Schiff bases as fixed carriers of oxygen, and oxygen permeability in ESBS membranes and oxygen-binding ability to the cobalt Schiff base, are studied. Due to the reversible absorption of oxygen by ESBS–CoS, the permeation of oxygen is observable for the lower upstream pressure and can be explained as a dual-mode process. The facilitation is enhanced in the polymeric complexed membrane by the higher oxygen dissociation constant and the lower crystallinity of the ESBS–CoS membrane.

Introduction

Membranes for gas separation have received much attention since membrane processes have the potential of being efficient.[1] Essential requirements for such membranes are high permeability and high permselectivity for a particular gas. When Robb[2] in 1967 reported the permeation properties of silicone rubber for a wide variety of gases and vapors, it was clear that rubber was a highly permeable polymer for most gases but that its permselectivity was low. Therefore much attention has been directed to modifying rubber for gas separation processes.[3-5]

Metal complexes, such as iron–porphyrin derivatives, form reversible oxygen adducts and have been successfully used as oxygen-transporting fluid membranes[6] and as an oxygen-separating liquid membrane.[7] Recently there has been considerable interest in the production of oxygen-enriched air by the use of a permselective membrane, which was prepared from a polymer complexed with the metal complex acting as a fixed carrier for oxygen permeation. In 1986, Nishide reported the preparation of polymer membranes containing cobalt complexes as fixed carriers of oxygen that absorb and transport oxygen selectively by the Langmuir mode.[8] Drago and Balkus also reported that the cobalt–*N*,*N*′-bis[(3-salicylideneamino)propyl]-methylamine complex bound to a polystyrene membrane enhances the selectivity for oxygen permeation through a polystyrene membrane at low pressures.[9] Sugia[10] reported a new preparative method for a thin polymer–metal complex membrane, which showed high O_2/N_2 permselectivity.

In our previous work the preparation of styrene–butadiene–styrene-*g*-vinyl pyridine graft copolymer (SBS-*g*-VP) by radiation-induced graft copolymerization and epoxidized styrene–butadiene–styrene copolymer (ESBS) by in situ epoxidation was studied.[11,12] The membranes of SBS-*g*-VP and ESBS were prepared by a solution casting method, and their performances in gas separation were discussed in detail.[12-16] It was found that the upstream gas pressure did not have any effect on the oxygen permeability of SBS-*g*-VP and ESBS membranes without (*N*,*N*′-disalicylideneethylenediamine)cobalt(II) (CoS1). But the effect was pronounced on the SBS-*g*-VP and ESBS membranes containing CoS1.[14-16] Such behavior might be explained by a dual-mode process.[17] Also in the previous studies,[15,16] the complex formation reactions of SBS-*g*-VP graft copolymer and ESBS with CoS1 in chloroform were studied quantitatively and the coordination number and formation constants were determined by the Miller method.[18] The polymeric complexed membranes, (SBS-*g*-VP–CoS1) and (ESBS–CoS1), were prepared by homogeneously complexing CoS1 to SBS-*g*-VP graft copolymer and to ESBS. It was found that the polymeric complexed membranes (SBS-*g*-VP–CoS1 and ESBS–CoS1) could react with molecular oxygen to form reversible oxygen adducts. The kinetics of the interaction of SBS-*g*-VP–CoS1 or ESBS–CoS1 membrane with molecular oxygen could be studied by UV and the equilibrium, association, and dissociation constants could be determined. Due to the reversible reactivity of oxygen binding to SBS-*g*-VP–CoS1 and ESBS–CoS1 membranes, the permeability of oxygen through SBS-*g*-VP–CoS1 and ESBS–CoS1 membrane can be explained by a dual-mode process.

In order to investigate the correlation between the facilitation of oxygen transport and oxygen-binding ability of metal complexes, four samples of cobalt Schiff bases (CoS) with different structures were prepared as oxygen carriers (Figure 1). Polymeric complexed membranes were prepared by homogeneously complexing cobalt Schiff base to ESBS. Then the reversibility of oxygen binding to the cobalt Schiff base in the ESBS membrane and the effect of the cobalt Schiff base on facilitated transport of oxygen were studied.

Experimental Section

Materials. The styrene–butadiene–styrene triblock copolymer (SBS) used was Kraton 1101 from the Shell Co. The characteristics of Kraton 1101 are listed in Table I. SBS was epoxidized as in the previous work[12] to form epoxidized styrene–butadiene–styrene block copolymer (ESBS). In this study, the oxirane weight content was 5.85% in ESBS and the concentration of ESBS was based on the concentration of oxirane. *N*,*N*′-Ethylenebis(salicylideneiminato)cobalt(II) and three different structure derivatives (Figure 1) were synthesized as in the literature.[19,20] The polymeric membranes complexed with cobalt Schiff base (CoS) were prepared by homogeneously complexing CoS to ESBS.[14-16]

Spectroscopic Measurements. Complex formation between ESBS and cobalt Schiff base in chloroform solution was observed to be accompanied by a spectral change in the visible absorption when measured with a Hitachi 320 spectrometer.

The ESBS–CoS membranes were prepared by solution casting, as in the previous work,[15,16] with thicknesses of 92 μm, and were kept in a vacuum oven at 50 °C for 1 day. The samples were then stored under different oxygen pressures. The changes in optical

0024-9297/91/2224-4010$02.50/0

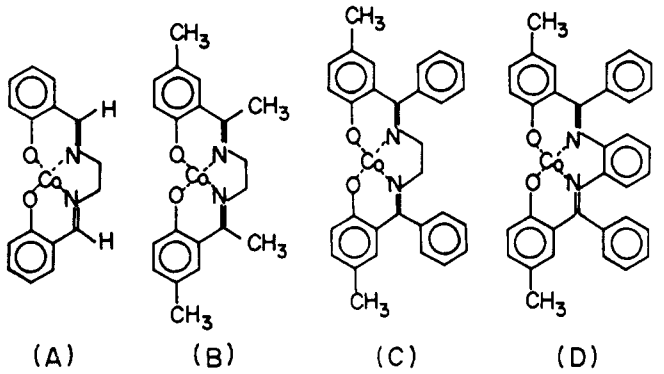

Figure 1. Names and structures of the cobalt Schiff base complex. (A) *N,N'*-ethylenebis(salicylideneiminato)cobalt(II) (CoS1), (B) *N,N'*-ethylenebis(3,7-dimethylsalicylideneiminato)-cobalt(II) (CoS2), (C) *N,N'*-ethylenebis(3-methyl-7-phenylsalicylideneiminato)cobalt(II) (CoS3), (D) *N,N'*-phenylenebis(3-methyl-7-phenylsalicylideneiminato)cobalt(II) (CoS4).

Table I
Molecular Characteristics of Kraton 1101

total molecular weight	102×10^3
polystyrene, %	33
terminal PS block, $\bar{M}_w$	17×10^3
central PB block, $\bar{M}_w$	68×10^3
microstructure	
PB 1,4-trans, %	42
PB 1,4-cis, %	49
PB 1,4, %	9

Table II
Optical Absorbance of Various Complexes in Chloroform

sample	max, nm	sample	max, nm
CoS1	418, 340	CoS3	424, 345
CoS2	420, 350	CoS4	400

Table III
Formation Constant for the ESBS–CoS Membrane

samples[a]	equilib const K, atm^{-1}	assoc const 10^3k_1, atm^{-1} min^{-1}	dissoc const 10^3k_2, min^{-1}
A	9.51	20.70	2.10
B	1.22	1.19	0.97
C	0.30	1.84	6.05
D	0.09	0.32	3.42

[a] A, oxygen binding to the complex in the ESBS–CoS1 membrane. B, oxygen binding to the complex in the ESBS–CoS2 membrane. C, oxygen binding to the complex in the ESBS–CoS3 membrane. D, oxygen binding to the complex in the ESBS–CoS4 membrane.

absorbance with various reaction times were measured at ~415 nm with a Hitachi 320 spectrometer. When the absorbance maintained a constant value, the equilibrium state was reached. The oxygen-binding equilibrium constant, association constant, and dissociation constant could be obtained from our kinetic studies.[15,16]

Studies of DSC Morphology and Gas Permeability of the ESBS–CoS Membrane. Differential scanning calorimetry (DSC, Du Pont 910 DSC) was performed. DSC scans were at 10 °C/min. The morphology of polymeric membranes was studied with a Nikon Microphot-Fx. Gas permeability through polymeric membrane is described in previous work.[15,16]

Results and Discussion

Complex Formation between ESBS and Cobalt Schiff Base. The optical absorbances of pure cobalt Schiff base in chloroform before the addition of ESBS were measured with a UV spectrophotometer. The results are shown in Table II. Successive addition of varying amounts of ESBS to a chloroform solution of CoS causes

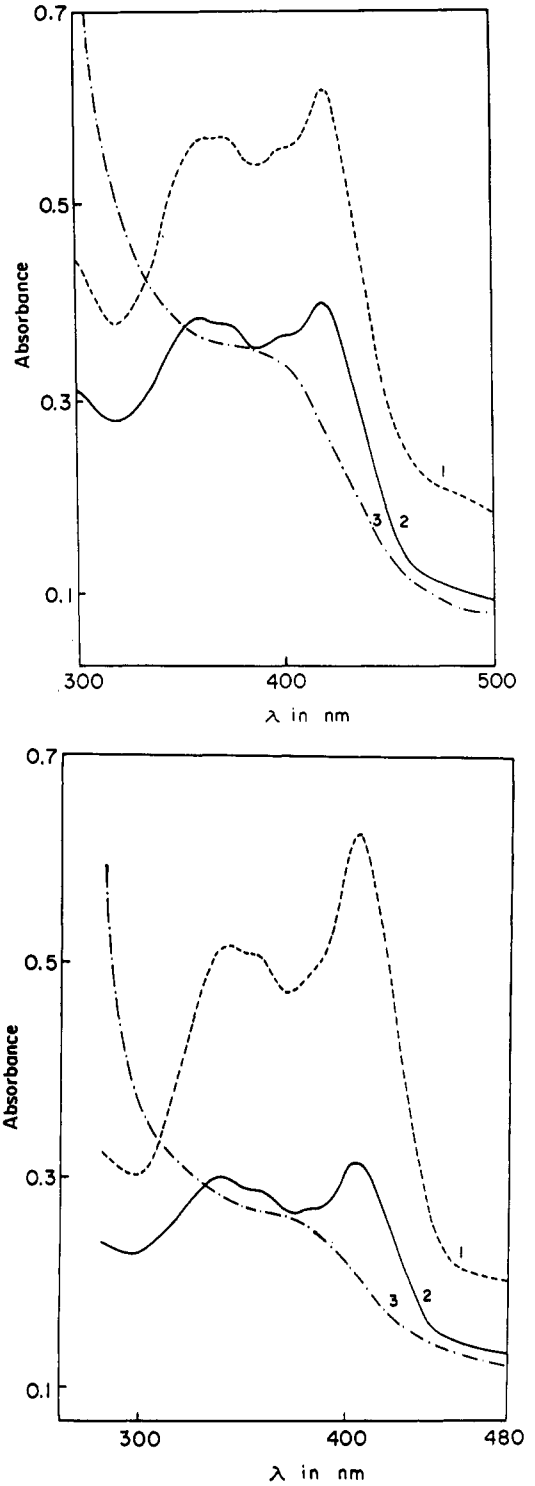

Figure 2. (a, top) Absorption spectra at 30 °C. Curves: (1) [ESBS] = 0 mol/L; (2) [ESBS] = 6.48×10^{-4} mol/L; (3) [ESBS] = 1.34×10^{-2} mol/L. [CoS2] = 6.86×10^{-5} mol/L in chloroform. (b, bottom) Absorption spectra at 30 °C. Curves: (1) [ESBS] = 0 mol/L; (2) [ESBS] = 2.36×10^{-3} mol/L; (3) [ESBS] = 1.34×10^{-2} mol/L. [CoS3] = 6.86×10^{-5} mol/L in chloroform.

a change in the absorption spectrum of the CoS. As shown in Figure 2, parts a and b, both absorption peaks of CoS2 and of CoS3 disappeared when excess ESBS was added. This is due to complex formation between ESBS and CoS as described in previous studies.[15,16]

Reversible Oxygen Binding to the Cobalt Schiff Base in the ESBS Membrane (ESBS–CoS). The optical absorbances of various ESBS–CoS polymeric complexed membranes under vacuum were measured. Various ESBS–CoS membranes were placed at different pressures

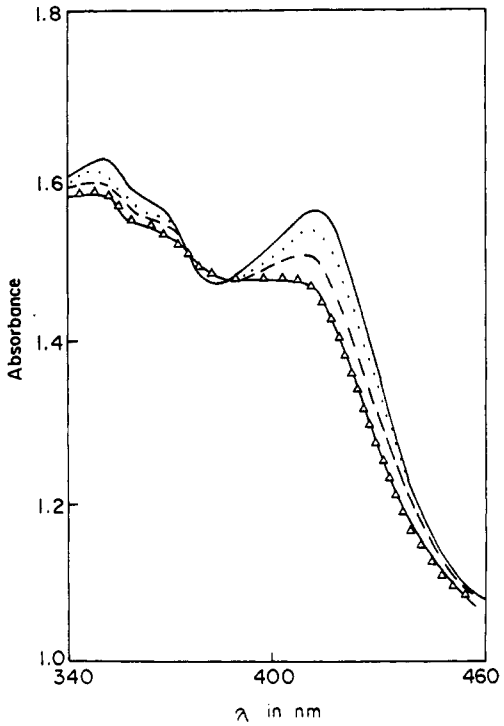

Figure 3. Absorption spectra of oxygen bound to ESBS–CoS membrane at 30 °C. For various times (t): t = 0 min (—); t = 10 min (···); t = 30 min (– –); t = 50 min, (Δ).

and the changes of the optical absorbance were measured with reaction time. As shown in Figure 3, the absorption peak decreased with reaction time. When the samples were placed under vacuum again, the optical absorption could be reversible. From the study of ESR in previous work,[14] the Co–O_2 adduct was observed even after the film was pumped under vacuum. This means that partial irreversible oxidation occurred. According to previous studies,[15,16] the oxygen-binding equilibrium constant ($K = k_1/k_2$), association constant (k_1), and dissociation constant (k_2) could be obtained from our kinetic methods for

$$\text{ESBS–CoS} + O_2 \underset{k_2}{\overset{k_1}{\rightleftharpoons}} \text{ESBS–CoS–}O_2 \qquad (1)$$

As shown in Table III, the K values of ESBS–CoS decrease as follows: ESBS–CoS1 > ESBS–CoS2 > ESBS–Co3 > ESBS–CoS4.

This might be due to a steric effect of the cobalt Schiff base. As shown in Figure 1, there are two phenyl group substituents in CoS3 and three phenyl group substituents in CoS4, so their K values are lower than those for CoS1 and CoS2. The dissociation constant of ESBS–CoS increases as follows: ESBS–CoS2 > ESBS–CoS1 > ESBS–CoS4 > ESBS–CoS3.

These results agree with the heats of dissociation of the ESBS–CoS membranes given in Table IV and Figure 4. As reported in previous work,[15] the endothermic peaks shown in Figure 4 resulted from the dissociation of oxygen bound to CoS in the ESBS–CoS membrane, because the binding interaction between oxygen and CoS was dominated by the steric effect and the readiness of electron release of this ligand. In Figure 1, CoS2 has a methyl group substituent, while CoS3 and CoS4 have phenyl group substituents. The phenyl group being a hard ring substituent, the steric effect is the highest for CoS4. This results in the weakest binding between oxygen and CoS. The order of electron release for methyl and phenyl groups

Table IV
Heat of Dissociation for the ESBS–CoS Membrane

sample[a]	$10^{-2}\Delta H$, J/g	T_i, °C
A	20.15	−2.46
B	39.58	2.20
C	11.50	−6.07
D	17.15	−3.23

[a] A, ESBS–CoS1 membrane treated in 1 atm oxygen, 2 days. B, ESBS–CoS2 membrane treated in 1 atm oxygen, 2 days. C, ESBS–CoS3 membrane treated in 1 atm oxygen, 2 days. D, ESBS–CoS4 membrane treated in 1 atm oxygen, 2 days.

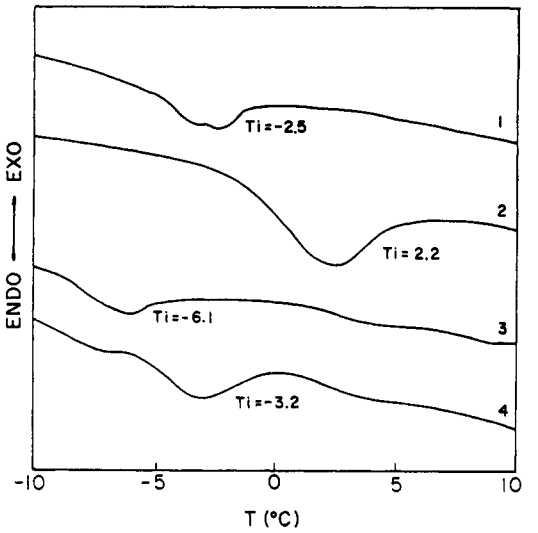

Figure 4. DSC thermograms (10 °C/min) for ESBS–CoS1 (1), ESBS–CoS2 (2), ESBS–CoS3 (3), and ESBS–CoS4 (4) membrane treated in 1 atm oxygen for 2 days.

Table V
Oxygen Binding Formation Constant at Various Temperatures for the ESBS–CoS1 Membrane

test temp, °C	equilib const K, atm^{-1}	assoc const 10^3k_1, atm^{-1} min^{-1}	dissoc const 10^3k_2, min^{-1}
30	9.5	20.70	2.1
40	3.7	30.20	8.2
50	1.6	40.20	25.1

Table VI
Thermodynamic Parameters for the ESBS–CoS1 Membrane

ΔE_1, kcal/mol	6.47
ΔE_2, kcal/mol	24.3
ΔH, kcal/mol	−17.8
ΔS, eu	−54.2

is $CH_3 > C_6H_5 > H$.[21] So the ligand of CoS2 donates electrons to Co(II) more significantly than the others, and as a result, the binding interaction between oxygen and CoS is the strongest. Table V shows that the association constant and dissociation constant of ESBS–CoS1 increases with temperature but the oxygen-binding equilibrium constant decreases. From a Van't Hoff plot, the thermodynamic parameters for ESBS–CoS1 were calculated and are listed in Table VI. This shows that oxygen binding to CoS1 in ESBS–CoS1 is an exothermic reaction. This is due to CoS1 being complexed with the oxygen atom of the oxirane ring of ESBS.[16] The hindrance for oxygen binding to CoS1 in the ESBS–CoS1 membrane is dominated by a steric effect. With increase of test temperature, the free volume of ESBS–CoS1 also increased. The diffusivity for oxygen through ESBS–CoS1 became easier, and association occurred more readily. Thus, the association constant increases with increasing test temperature.

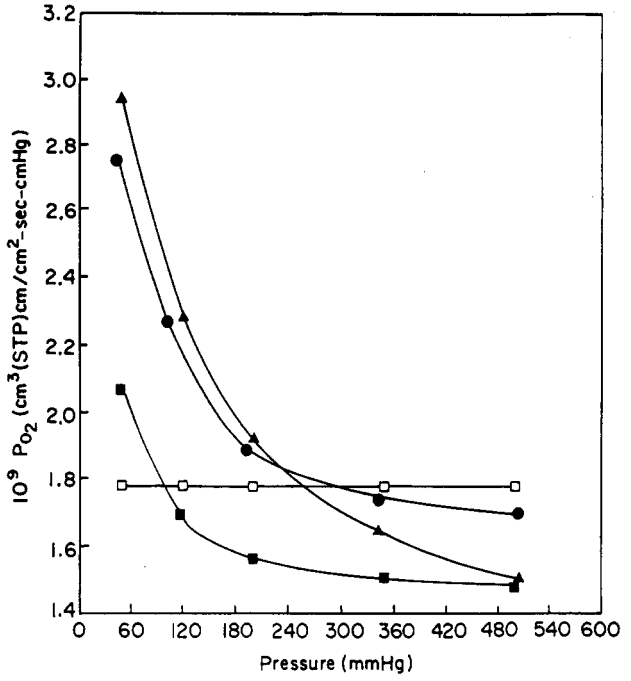

Figure 5. Effect of upstream gas pressure on permeation coefficients for the ESBS–CoS membrane [oxygen at CoS2 (●), CoS3 (▲), and CoS4 (■)] and the ESBS membrane [oxygen (□) at 30 °C].

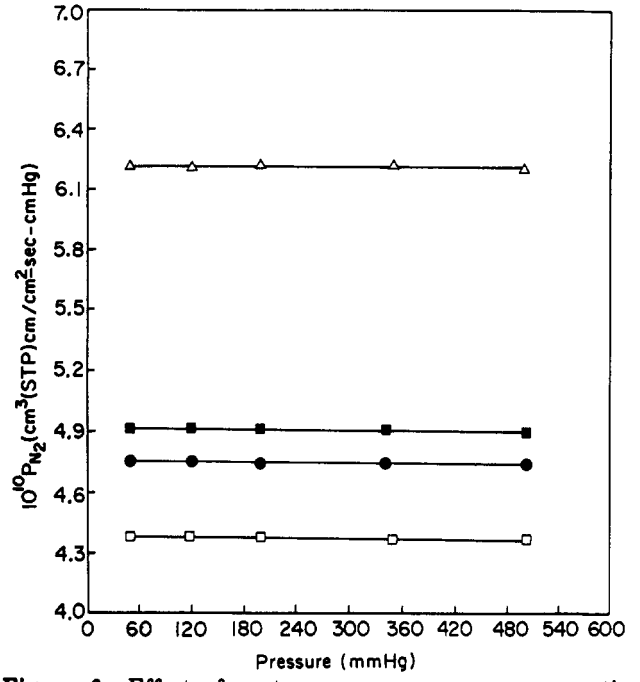

Figure 6. Effect of upstream gas pressure on permeation coefficients for the ESBS–CoS membrane [nitrogen at CoS2 (■), CoS3 (●), and CoS4 (□)] at 30 °C and the ESBS membrane [oxygen (△) at 30 °C].

Effect of Cobalt Schiff Base on Facilitated Transport of Oxygen. Figures 5 and 6 show the effect of upstream gas pressure (p_2) on the permeability coefficients (P_{O_2} and P_{N_2}) in an ESBS membrane containing 3.56×10^{-5} mol of CoS. P_{O_2} increases with a decrease in p_2 for ESBS containing CoS. P_{N_2} is independent of p_2 because the oxygen carrier does not interact with nitrogen. This is also supported by the fact that P_{O_2} is independent of p_2 for an ESBS membrane not containing CoS. This is a result of the affinity of ESBS–CoS for absorbing oxygen reversibly. This suggests that oxygen transport occurs by a dual-mode process[8,17] mechanism (Henry mode and additive Langmuir mode); i.e., P_{O_2} is equal to the sum of the first term, the Henry mode, and the second term, the Langmuir mode:

$$P_{O_2} = K_D D_D + \frac{D_C C_C K}{1 + K p_2} \quad (2)$$

where P_{O_2} is the oxygen permeability through ESBS–CoS, k_D is the solubility coefficient for Henry's law, D_D and D_C are the diffusion coefficients for Henry-type and Langmuir-type diffusions, respectively, C_C is the saturated amount of oxygen reversibly bound to the binding site, K is the oxygen-binding and dissociation equilibrium constant, and p_2 is the upstream gas pressure.

As reported in previous work,[14] when the cobalt was nearly completely oxygenated, O_2 was not removed from the low-pressure side of the film and the driving force for facilitated transfer of O_2 to the surface was removed. The O_2 adduct then inhibited the permeation through the film, in comparison to the ESBS membrane without CoS, by removing free volume. Therefore the permeability of O_2 for the ESBS membrane without CoS was higher than that of the ESBS membrane containing CoS, when the upstream gas pressure was over 300 mmHg. This means that the steric effect is very important for oxygen to pass through ESBS–CoS membranes. This is confirmed by Figure 7. A crystallite structure was found in the ESBS–CoS4 membrane, resulting in the lowest permeability. When the upstream gas pressure was lower than 200 mmHg, the P_{O_2} value decreased as follows: ESBS–CoS3 > ESBS–CoS2 > ESBS–CoS4. This is one of the indications that the character of the oxygen carrier is critically reflected in the oxygen permeation behavior and could be explained as follows. (1) For high K values a large part of the Langmuir site, i.e., the CoS, is occupied by molecular oxygen; however, if the k_2 value is low, the absorbed oxygen is difficult to dissociate from the site (Table III). (2) The P_{O_2} value was dominated by the Henry mode and the Langmuir mode. Because crystallinity is a great hindrance for gas to pass through the membrane, the decrease of P_{O_2} for the Henry mode will be very significant for ESBS–CoS4 and this is in agreement with the P_{N_2} value as shown in Figure 6. From both effects as described above, the P_{O_2} value is ESBS–CoS3 > ESBS–CoS2 > ESBS–CoS4 at upstream gas pressures lower than 200 mmHg.

The time lag for oxygen permeation (θ_{O_2}) also depended on p_2 in the same manner as the permeation coefficient, as shown in Figure 8. This behavior indicates that oxygen clearly interacts with CoS in the ESBS–CoS membrane. This is further supported by the fact that the time lag for nitrogen permeation (θ_{N_2}) in the ESBS–CoS membrane (Figure 9) and the time lag for oxygen permeation (θ_{O_2}) in the ESBS membrane without CoS (Figure 8) are independent of the upstream gas pressure. As shown in Figure 8, the time lag for oxygen permeation in the ESBS–CoS membrane decreased as follows: ESBS–CoS4 > ESBS–CoS2 > ESBS–CoS3 > ESBS. The reasons for the time lag are the same as for the oxygen permeation coefficient differences in the ESBS–CoS membrane. (1) Crystallinity will decrease gas diffusivity and result in a long term lag; (2) the larger oxygen affinity (K) and smaller oxygen kinetic dissociation constant (k_2) of ESBS–CoS result in a more prolonged time lag. Combining both effects, the time lag for oxygen permeation in membranes is ESBS–CoS4 > ESBS–CoS2 > ESBS–CoS3 > ESBS. Due to the hard phenyl group of CoS4 and CoS3, the steric effect will be significant if CoS3 and CoS4 are added to the ESBS membrane and will result in a significant decrease of the

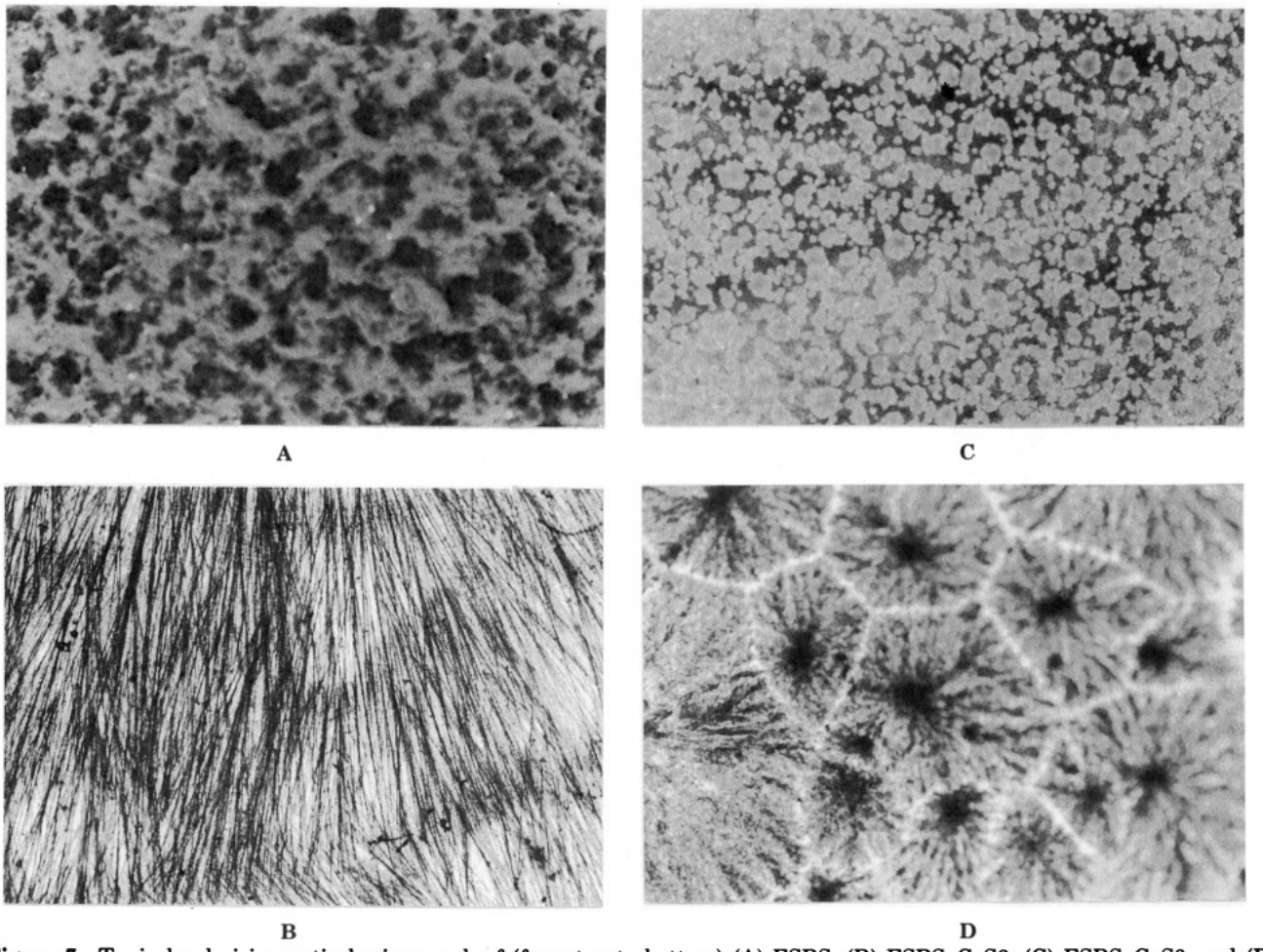

Figure 7. Typical polarizing optical micrograph of (from top to bottom) (A) ESBS, (B) ESBS–CoS2, (C) ESBS–CoS3, and (D) ESBS–CoS4 (magnification ×26).

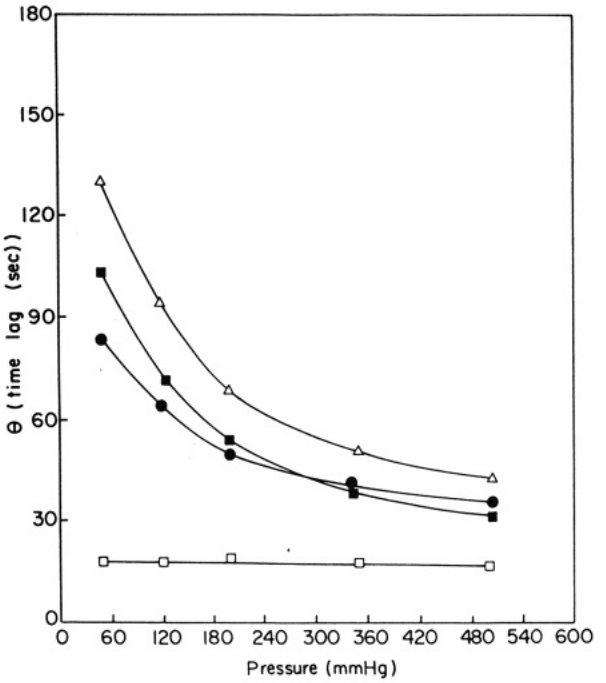

Figure 8. Effect of upstream gas pressure on the time lag for the ESBS–CoS membrane [oxygen at CoS2 (■), CoS3 (●), and CoS4 (△)] at 30 °C and the ESBS membrane [oxygen (□) at 30 °C].

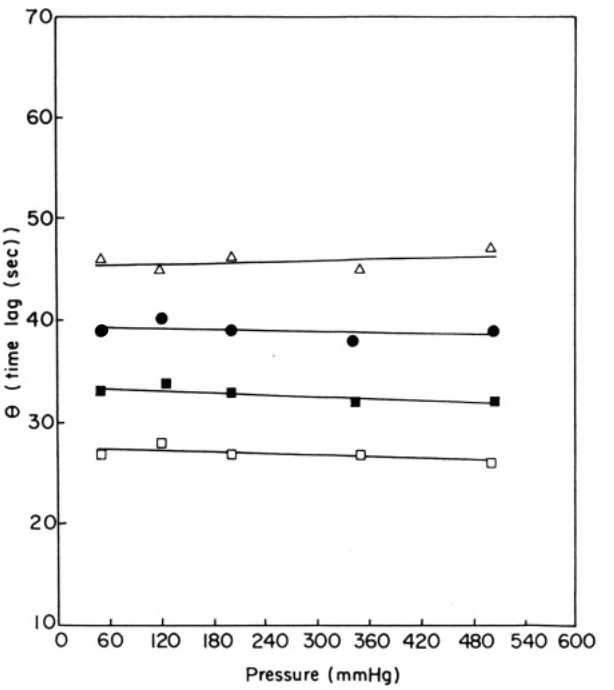

Figure 9. Effect of upstream gas pressure on the time lag for the ESBS–CoS membrane [nitrogen at CoS2 (■), CoS3 (●), and CoS4 (△)] at 30 °C and the ESBS membrane [oxygen (□) at 30 °C].

free volume of the ESBS–CoS membrane. From the viewpoint of free volume theory, CoS4 and CoS3 in the ESBS membrane was very rigid and dispersed in the matrix of ESBS, as shown in Figure 7. So the time lag for nitrogen permeation in ESBS–CoS membrane is ESBS–CoS4 > ESBS–CoS3 > ESBS–CoS2 > ESBS (Figure 9). This is

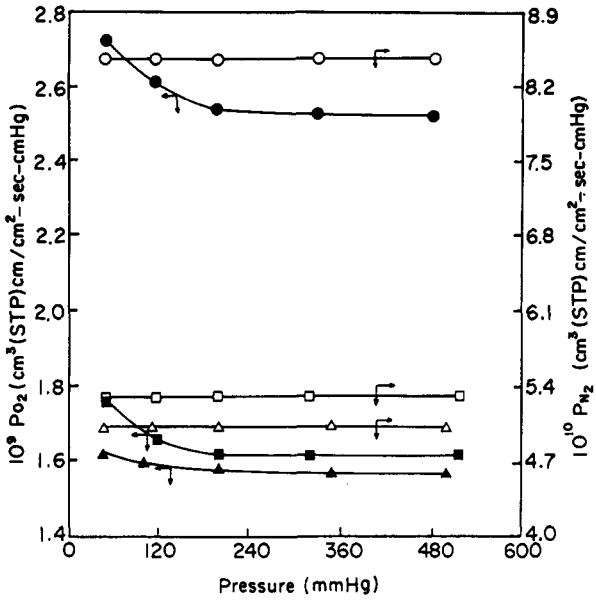

Figure 10. Effect of upstream gas pressure on permeation coefficients of the ESBS–CoS1 membrane [oxygen at 30 (▲), 40 (■), and 50 °C (●); nitrogen at 30 (△), 40 (□), and 50 °C (○)].

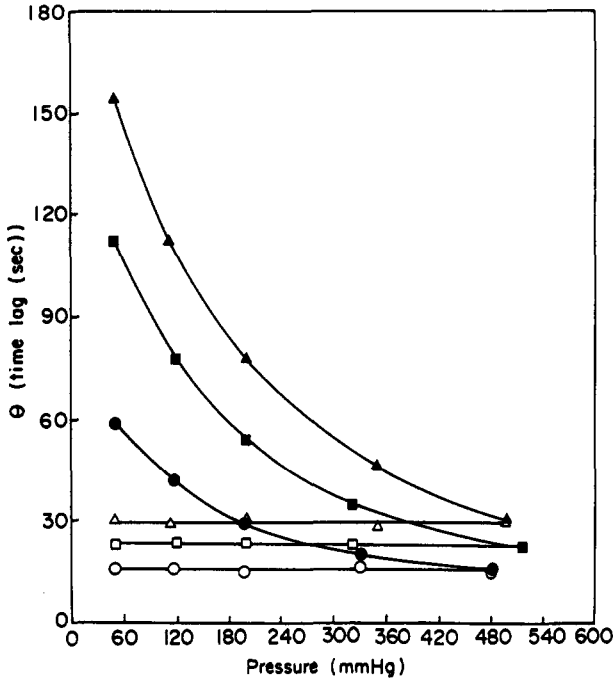

Figure 11. Effect of upstream gas pressure on the time lag of the ESBS–CoS1 membrane [oxygen at 30 (▲), 40 (■), and 40 °C (●); nitrogen at 30 (△), 40 (□), and 50 °C (○)].

the same reason why the permeability of nitrogen in the ESBS–CoS membrane is ESBS > ESBS–CoS2 > ESBS–CoS3 > ESBS–CoS4.

Figure 10 shows that permeability coefficients (P_{O_2} and P_{N_2}) and the p_2 dependence of P_{O_2} increase with temperature. Figure 11 shows the time lag for oxygen and nitrogen permeation (θ_{O_2} and θ_{N_2}) and the p_2 dependence on θ_{O_2} decrease with temperature. P_{N_2} increases and θ_{N_2} decreases with temperature. This may be due to the increase of moving velocity and free volume of the ESBS–CoS1 membrane. It is the same reason for P_{O_2} and θ_{O_2}, and the p_2 dependence of P_{O_2} and θ_{O_2} are based on oxygen binding to CoS1. From Table V, the oxygen dissociation constant (k_2) increases with temperature but the oxygen-binding equilibrium constant decreases with increasing temperature.

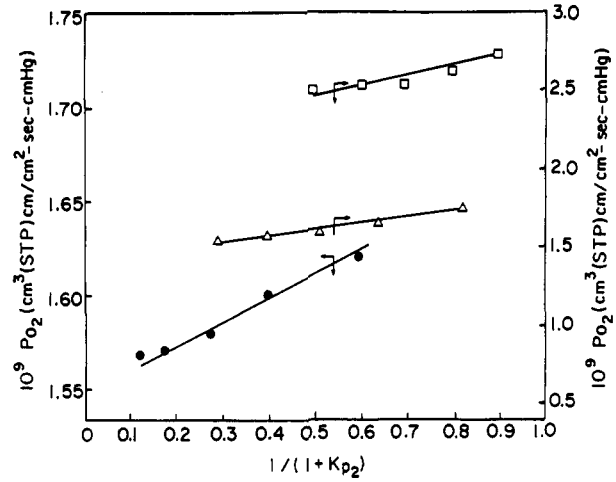

Figure 12. Oxygen permeability in the ESBS–CoS1 membrane plotted according to eq 2 at 30 (●), 40 (△), and 50 °C (□).

Table VII
Permeability for Various Samples and Operating Conditions

polymer[a]	oxygen carrier	$10^9 P_{O_2}$	selectivity (P_{O_2}/P_{N_2})	pressure, mmHg	temp, °C	ref
ESBS		1.78	2.9	50	30	*b*
ESBS	CoS3	2.94	6.2	50	30	*b*
ESBS	CoS4	2.10	4.5	50	30	*b*
POMPY		1.95	2.3	10	35	22
POMPY	CoS1	2.65	4.8	10	35	22
PBMA		0.64	3.2	5	25	8
PBMA	CoP1	1.20	5.7	5	25	8
PIMS	CoP1	0.68	3.6	50	30	23

[a] POMPY, poly[(octyl methacrylate)-*co*-(4-vinylpyridine)], PBMA, poly(butyl methacrylate), PIMS, poly[dimethylsiloxane–[3-(1-imidazolyl)propyl]siloxane], CoP1 [α,α,α,α-*meso*-tetrakis(*o*-pivalamidophenyl)porphinato]cobalt(II)–1-methylimidazole, CoP2, 3,6-diazaoctamethylenediamine. [b] This work.

Due to the effect of oxygen-binding ability, P_{O_2} and θ_{O_2} significantly depend on p_2. This is the difference between P_{O_2}, θ_{O_2} and P_{N_2}, θ_{N_2}. The effect of p_2 on P_{O_2} was analyzed by eq 2; that is, P_{O_2} was plotted against $1/(1+Kp_2)$ (Figure 12). It is confirmed that a dual-mode process is suitable to explain the oxygen transport through an ESBS–CoS membrane within our test temperature range.

Table VII shows (1) the oxygen permeability and the O_2/N_2 selectivities are improved with an oxygen carrier and (2) the performance of the ESBS–CoS3 membrane is better than the others. From the above discussion, the oxygen-binding affinity of the oxygen carrier is very important for oxygen transport in a polymeric complexed membrane containing an oxygen carrier. However, the difference of P_{O_2} and O_2/N_2 selectivity is due to different carrier properties induced by different in-plane (equatorial) ligands. In a subsequent paper, the effect of different axial ligands and cast solvent on facilitated oxygen transport will be discussed.

Acknowledgment. This work was supported by the National Science Council of the Republic of China under Grant NSC-80-0405-E007-01.

References and Notes

(1) For review, see: (a) Lonsdale, H. K. *J. Membr. Sci.* **1982**, *10*, 81. (b) Puskch, W.; Walch, A. *Angew. Chem., Int. Ed. Engl.* **1982**, *21*, 660. (c) Strathmenn, H. *J. Membr. Sci.* **1981**, *9*, 121.
(2) Robb, W. L. *Ann. N.Y. Acad. Sci.* **1967**, *146*, 119.
(3) Ward, W. J., III; Browall, W. R.; Salemme, R. M. *J. Membr. Sci.* **1976**, *1*, 99.

(4) Kawakami, M.; Yamashita, Y.; Iwamoto, M.; Kagawa, S. *J. Membr. Sci.* **1984**, *19*, 249.
(5) Springmann, D. H. *CEER, Chem. Econ. Eng. Rev.* **1982**, *14*, 17.
(6) (a) Tsuchida, E. *J. Macromol. Sci., Chem.* **1979**, *A13*, 545. (b) Tsuchida, E. Nishide, H.; Yuasa, M.; Hasegawa, E., Matsushita, Y.; Eshima, K. *J. Chem. Soc., Dalton Trans.* **1985**, 275. (c) Tsuchida, E. *Ann. N.Y. Acad. Sci.* **1985**, *446*, 429.
(7) Roman, I. C.; Baker, I. W. Eur. Patent 98731, 1983.
(8) (a) Nishide, H.; Ohyanagi, M.; Okada, O.; Tsuchida, E. *Macromolecules* **1986**, *19*, 494. (b) Nishide, H.; Ohyanagi, M.; Okada, O.; Tsuchida, E. *Macromolecules* **1987**, *20*, 417.
(9) Drago, R. S.; Balkus, K. J. *Inorg. Chem.* **1986**, *25*, 716.
(10) Sugia, K. *Polym. Mater. Sci. Eng.* **1988**, *59*, 139.
(11) Yang, J. M.; Hsiue, G. H. *J. Appl. Polym. Sci.* **1990**, *39*, 1475.
(12) Hsiue, G. H.; Yang, J. M. *J. Polym. Sci., Polym. Chem. Ed.* **1990**, *28*, 3761.
(13) Yang, J. M.; Hsiue, G. H. *Angew. Makromol. Chem.* **1990**, *179*, 99.
(14) Yang, J. M.; Hsiue, G. H. *J. Appl. Polym. Sci.* **1990**, *41*, 1141.
(15) Yang, J. M.; Hsiue, G. H. *J. Polym. Sci., Polym. Chem. Ed.*, in press.
(16) Hsiue, G. H.; Yang, J. M.; Lee, P. S.; Liaw, C. Y. *J. Polym. Sci., Polym. Chem. Ed.* **1990**, *28*, 3363.
(17) Paul, D. R.; Koros, W. J. *J. Polym. Sci., Polym. Phys. Ed.* **1976**, *14*, 675.
(18) Miller, J. R.; Dorough, G. D. *J. Am. Chem. Soc.* **1952**, *74*, 3977.
(19) Bailes, R. H.; Calvin, M. *J. Am. Chem. Soc.* **1947**, *69*, 1896.
(20) Basolo, F. *Acc. Chem. Res.* **1975**, *8*, 384.
(21) McMurry, J. *Organic Chemistry*; Brooks/Cole Publishing Co.: Pacific Grove, CA.
(22) Tsuchida, E.; Nishide, H.; Ohyanagi, M.; Kawakami, H. *Macromolecules* **1987**, *20*, 1907.
(23) Nishide, H.; Ohyanagi, M.; Suenaga, K.; Tsuchida, E. *J. Polym. Sci., Polym. Chem. Ed.* **1989**, *27*, 1439.

Registry No. O_2, 7782-44-7.